

# Flow, Ordering and Jamming of Sheared Granular Suspensions

Denis S. Grebenkov,<sup>1,2,\*</sup> Massimo Pica Ciamarra,<sup>3,1</sup> Mario Nicodemi,<sup>1,4</sup> and Antonio Coniglio<sup>1</sup>

<sup>1</sup>*Dip.to di Scienze Fisiche, Università di Napoli "Federico II" and INFN, Naples, ITALY*

<sup>2</sup>*LPMC, C.N.R.S. – Ecole Polytechnique, F-91128 Palaiseau, FRANCE*

<sup>3</sup>*CNISM & Dip.to of Information Engineering, Seconda Università di Napoli, Aversa, ITALY*

<sup>4</sup>*Complexity Science & Department of Physics, University of Warwick, UK*

(Dated: Received: February 27, 2008/ Revised version:)

We study the rheological properties of a granular suspension subject to constant shear stress by constant volume molecular dynamics simulations. We derive the system ‘flow diagram’ in the volume fraction/stress plane  $(\phi, F)$ : at low  $\phi$  the flow is disordered, with the viscosity obeying a Bagnold-like scaling only at small  $F$  and diverging as the jamming point is approached; if the shear stress is strong enough, at higher  $\phi$  an ordered flow regime is found, the order/disorder transition being marked by a sharp drop of the viscosity. A broad jamming region is also observed where, in analogy with the glassy region of thermal systems, slow dynamics followed by kinetic arrest occurs when the ordering transition is prevented.

PACS numbers: 45.70Vn, 83.50.Ax, 83.10.Tv

Keywords: granular suspension, kinetic arrest, jamming, order/disorder transition

Under the effects of external drives granular media exhibit a variety of complex dynamical behaviors. Compaction under shaking is a well studied phenomenon, characterized by slow relaxation followed by a jamming transition at high volume fraction [1, 2, 3] with deep analogies to thermal glasses [2, 3, 4, 5]. In addition shear-induced transitions from flowing to jammed states [6] or to ordered flowing states are observed [7, 8]. In such a complex panorama, the rheology of the different phases of a system under shear is far from being clarified, and even a clear ‘flow diagram’ locating the regions with ordered flow, disordered flow, and jamming, is missing.

Within such a perspective, we investigate by molecular dynamics (MD) simulations the rheology of a dense granular suspension subject to a constant shear stress in a box of constant volume. Alike previous experiments on non-Brownian particles (see [9, 10] and references therein), we opt for a constant shear stress rather than a constant shear rate setup (see [8] and references therein) because jamming may be precluded in the latter case. We derive the system ‘flow diagram’ as obtained by shearing for a long time a disordered assembly of grains. It includes an order/disorder transition line, signaled by a sharp drop of the effective viscosity  $\eta$ , as well as a jamming region. Similarly to supercooled liquids, a crossover from a transient disordered flow to a stationary ordered one is also found, jamming occurring when ordering is kinetically impeded. In the regime of disordered flow, the system viscosity,  $\eta$ , is found to grow with the applied shear stress according to Bagnold scaling, but it departs from it when the shear stress increases. As the packing fraction grows towards a critical value,  $\eta$  is found to diverge with a power law. We also show that, similarly to glassy thermal systems, the long time state of the system in the jamming region is dependent on the dynamical preparation protocol.

We consider monodisperse spherical beads of diameter

$d$  and mass  $m$ , initially randomly located between the upper and lower plates of a box of a given size  $l_x \times l_y \times l_z$ . The lower plate is immobile and the upper one may move along  $x$  in response to a given applied shear stress  $\sigma$ , i.e., under a constant force  $F = \sigma l_x l_y$  (periodic boundary conditions are used along the  $x$  and  $y$  axes). Grains are studied by MD simulations of a well known linear spring-dashpot model (L3 of Ref. [11]), including particle rotations and static friction: normal interaction between two beads is characterized by the elastic and viscoelastic constants  $k_n = 2 \cdot 10^5$  and  $\gamma_n = 50$ , given in standard units [12]; static friction is implemented by keeping track of the elastic shear displacement throughout the lifetime of a contact. The tangential elastic constant is  $k_t = 5.7 \cdot 10^4$ ; the static friction coefficient  $\mu = 0.1$ ; the restitution coefficient is 0.88. The box top and bottom plates are made of spherical beads, randomly ‘glued’ at height  $z = l_z - 1/2 + \varepsilon$  and at  $z = 1/2 + \varepsilon$ , respectively, where  $\varepsilon$  is randomly chosen for each bead in the set  $[-1/4, 1/4]$ . The area fraction of grains on the plates is high (large non-physical overlaps are allowed between the constituent particles) and their mass is  $300m$ . We explored a range of box sizes, and below we illustrate the results by considering the case with  $l_x = l_y = 16$ , and  $l_z = 8$  where finite size effects are absent. The small value of  $l_x$  and  $l_y$ , taken here to allow simulations on time scales long enough, is partially compensated by our periodic boundary conditions ( $l_z$  has a value typical for experiments [7, 8, 10]). To avoid gravity-induced compaction, gravitational acceleration of grains is neglected as in density-matching liquid experiments [10].

For each value of the grain volume fraction  $\phi$  and of the applied force  $F$  we have performed 10 simulations using different initial disordered states, always finding the same typical velocities as well as the same long time state (we have performed simulations up to  $t = 8000$ ): the sys-

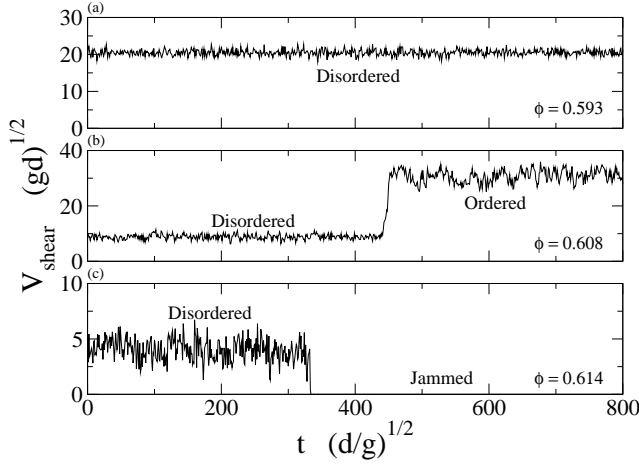


FIG. 1: Velocity of the system upper plate,  $v_{\text{shear}}$ , as a function of time,  $t$ , for the shown values of the volume fraction,  $\phi$ , sheared with a constant force  $F = 4 \cdot 10^4$ . The system starts from a disordered initial pack. **Panel (a)** When  $\phi$  is small enough the system flows in a disordered configuration (see text and Fig. 2 left panel). **Panel (b)** When  $\phi$  is increased the disordered flow is only transient, as the system has an abrupt transition to an ordered flow with a reduced viscosity (see text and Fig. 2 right panel). **Panel (c)** At even higher  $\phi$  the transient disordered flow has a transition to a jammed configuration where  $v_{\text{shear}} = 0$ .

tem rheology is therefore characterized by the value of  $F$  and on  $\phi$  (or equivalently on grain number  $N$  [19]). In the  $\phi$  and  $F$  range of values we explored, which is close to the hard-particle limit as the maximum deformation of a particle is  $\delta d/d < 10^{-2}$ , three qualitatively different regimes are usually observed in the system dynamics, corresponding to different behaviors of the measured upper plate velocity,  $v_{\text{shear}}(\phi, F)$ . They are summarized in Fig. 1 which shows  $v_{\text{shear}}$  as a function of time,  $t$ , at increasing values of the volume fraction,  $\phi = 0.593, 0.608$  and  $0.614$ , for  $F = 4 \cdot 10^4$ .

When  $\phi$  is small enough (Fig. 1a), the system flows in a stationary disordered state (as the one depicted in the left panel of Fig. 2) from the initial random configuration and  $v_{\text{shear}}$  fluctuates around a constant value depending on  $\phi$  and  $F$ . The degree of ordering of the system is usually quantified by the amplitude of the peak of the structure factor  $S(k)$  for, say,  $k = (0, 0, 2\pi/d)$ ; in the disordered region,  $S(k)$  has no peaks at all and takes values typical to disordered arrangements, as shown in Fig. 5b.

At higher  $\phi$  values, when  $F$  is strong enough (Fig. 1b), the system is trapped for a certain time in a transient state where  $v_{\text{shear}}$  keeps a constant value up to a moment when it suddenly jumps to a higher stationary plateau. Correspondingly, the system exits the disordered flowing state (left panel of Fig. 2) and develops a layered and partially ordered structure (shown in the right panel of Fig. 2).

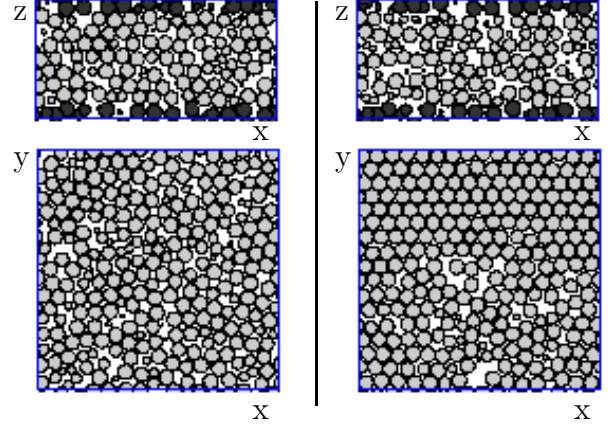


FIG. 2: Vertical ( $ZX$ , top) and horizontal ( $YX$ , bottom) snapshots of sections of the system for the run of Fig. 1b. The left and the right panels show sections taken at  $t = 400$ , when the system flow is disordered, and at  $t = 800$ , when the flow is ordered. The ordered state is characterized by the formation of crystal-like layers in the  $XY$  plane, shifted along  $z$ . Dark beads form the boundaries (the shown circles have various sizes as they are different cuts of our monodisperse spheres).

The high  $\phi$  scenario is drastically changed if the driving force  $F$  is not strong enough (see Fig. 1c): after a transient flow the system jams in a state as disordered as the initial one, and the upper plate velocity becomes zero. The above observations highlight that disordered states can be either stationary, or transient. The latter states can undergo transitions towards ordered flowing states, signalled by a marked increase of the shear velocity, or alternatively freeze towards jammed packs.

As the velocity profiles appear to be approximately linear in the considered cases, the system resistance to flow can be quantified via an effective viscosity  $\eta = F/v_{\text{shear}}(\phi, F)$ . In Fig. 5c we depict the ‘flow diagram’ of the suspension in the  $(\phi, F)$ -plane. We first consider the flow in the disordered region. Figure 3 shows the dependence of the effective viscosity on the applied shear force  $F$ , for several values of the volume fraction of the system,  $\phi$ . At low  $\phi$  and small applied shear stress, the viscosity increases to a good approximation with a power law,  $\eta \propto F^\alpha$ , where the exponent is  $\alpha \simeq 0.5$ . Accordingly, the relation between shear stress ( $\sigma \propto F$ ) and shear rate ( $\dot{\gamma} \propto v_{\text{shear}}$ ) is  $\sigma \propto \dot{\gamma}^\beta$ , with  $\beta = 1/(1 - \alpha) \simeq 2$ , in good agreement with the prediction of Bagnold scaling ( $\beta = 2$ ).

Within the disordered region, for a given force  $F$ , the dynamics of the system strongly slows down as  $\phi$  increases. This is apparent from Fig. 4 where we show that, at constant  $F$ , the effective viscosity diverges with a power law  $\eta(\phi) \propto (\phi_c(F) - \phi)^{-b}$  as the packing fraction increases. Such a relation recorded in the disordered regime anticipates the presence of a jamming critical vol-

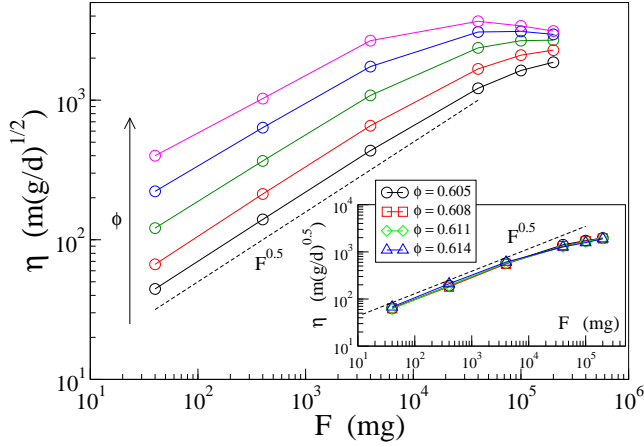


FIG. 3: The effective viscosity,  $\eta = F/v_{\text{shear}}(F)$ , as a function of the applied external force  $F$  for different values of the sample volume fraction ( $\phi = 0.573 - 0.619$ ), recorded in the disordered flow regime. At small  $F$  the viscosity increases, at a good approximation, as a power law in  $F^\alpha$ , with  $\alpha \simeq 0.5$ , which implies Bagnold scaling  $\sigma \propto \dot{\gamma}^\beta$ , with  $\beta \simeq 2$ . **Inset:** A similar power law scaling is found for  $\eta(F)$  in the ordered flow regime, but almost no dependence with  $\phi$  is observed.

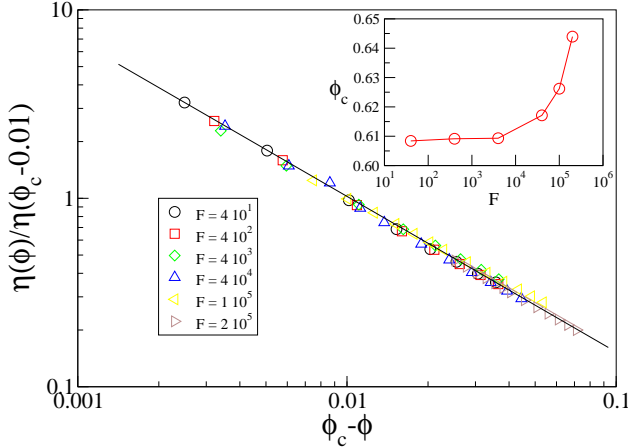


FIG. 4: At a given force  $F$ , the effective viscosity measured in the disordered flow regime diverges as a power law as the volume fraction of the sample approaches a jamming critical threshold  $\phi_c(F)$ . Interestingly, data collected at several  $F$  values collapse on a master power law, suggesting that its exponent is  $F$  independent. Here, we have scaled the data in such a way that  $\eta(\phi_c - 0.01) = 1$ . **Inset:** the fitted value to the critical volume fraction,  $\phi_c$ , increases with the applied external shear force.

ume fraction  $\phi_c(F)$  (see Fig. 4, inset). Interestingly, the fit of  $\phi_c(F)$  from the small  $\phi$ -value region always overestimates the volume fraction where we indeed observe the system to jam (see Fig. 5), in analogy to glass forming materials [13]. Fig. 4 also shows that data recorded at different  $F$  collapse one onto the other when plotted as

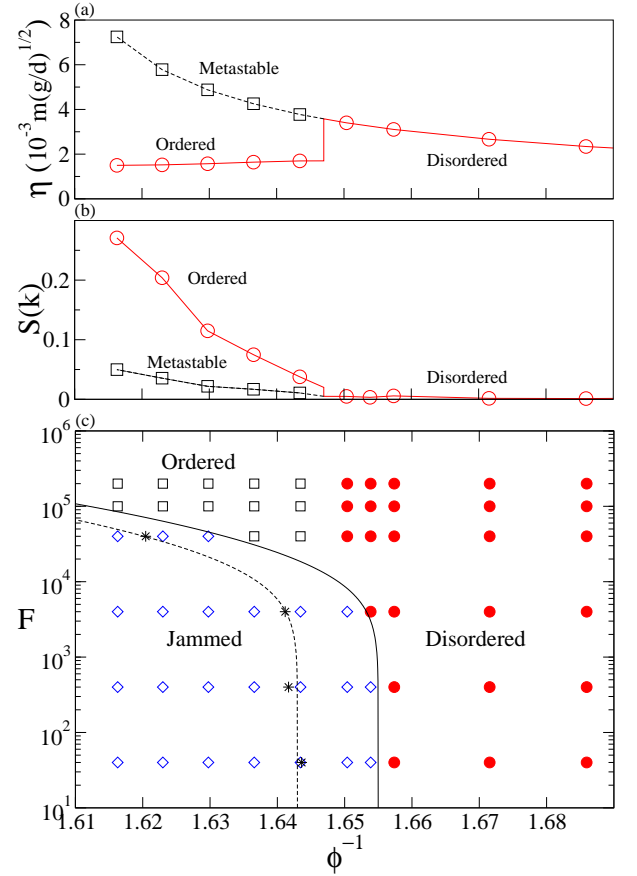


FIG. 5: **Panel (a)** and **(b)** show the dependence of the effective viscosity  $\eta$  and of the structure factor  $S(k)$  (for  $k = (0, 0, 2\pi/d)$ ) on the inverse volume fraction,  $\phi^{-1}$ , for  $F = 10^5$ . In the low  $\phi$  regime the system flow is disordered as  $S(k)$  has typically small values. By increasing  $\phi$ , there is an initial transient disordered flow ( $S(k)$  small) with growing  $\eta$ , followed by a sharp transition to an ordered flow (with a much higher  $S(k)$ , see text) with a sharp drop in the viscosity (see Fig. 1b). **Panel (c):** The system ‘flow diagram’ showing the long time flow regime as a function of the inverse volume fraction  $\phi^{-1}$  and of the applied force  $F$ : circles mark the region of disordered flow, open squares mark ordered flow, and diamonds the jammed region. Stars indicate the inverse critical volume fraction  $\phi_c^{-1}$  defined from the fit in Fig. 4.

a function of  $\phi_c(F) - \phi$ , suggesting that the exponent  $b \simeq 0.8$  is independent of  $F$ . This kind of power law dependence is frequently found in colloidal systems under shear [16], with the exponent  $b$  varying between 1 and 2.

We now consider the regime observed at higher  $\phi$  where, under shearing, the viscosity exhibits a sharp transition from a disordered to a faster ordered flow as in Fig 1b. The change to the faster flow, with the corresponding reduction of the effective viscosity, is associated to the formation of partially ordered layers parallel to the shearing plate (Fig. 2), as previously observed in experiments on granular and colloidal suspensions [8, 14, 15].

The connection between ordering and viscosity reduction is apparent in Fig. 5a,b, where we show the dependence of both  $\eta$  and  $S(k)$  on the inverse volume fraction of the system (squares indicate values recorded in the transient regime, circles the asymptotic ones). In the low  $\phi$  region, before the ordering transition,  $S(k)$  has small values typical to disordered arrangements. At higher  $\phi$ , the system can flow disordered, with increasing viscosity and  $S(k)$  having still comparable small values. Eventually, when a sharp drop in the viscosity is observed, it is accompanied by a clear increase of the structure factor  $S(k)$ , pointing out the presence of order in the system, as seen in the right panel of Fig. 2. In the ordered flow region,  $\eta$  is almost insensitive to  $\phi$  in the range here explored (see Fig. 5a) and has an approximate Bagnold-like scaling in  $F$ ,  $\eta \propto F^\alpha$ , with  $\alpha \simeq 0.5$  (see inset in Fig. 3). In the high  $\phi$  regime, if the applied shear stress is not strong enough, the initial transient disordered flow does not generally result in an ordered stationary flow, since a full dynamical arrest (see Fig. 5c) with  $v_{\text{shear}} = 0$  is found. Jamming occurs when the system disordered configurations are kinetically trapped in states where further shear (at the given value of  $F$ ) becomes impossible, the underlying mechanism being still unclear [17, 18]. Such a trapping is broken when  $F$  is high enough and ordered flow appears.

The flow diagram of Fig. 5c summarizes the properties of the long time states reached by the system when the initial condition is disordered, and suggests an analogy between the  $(\phi, F)$  flow diagram and the  $(\phi, T)$  phase diagram of usual thermal systems, the disordered, ordered and jammed states corresponding respectively to the liquid, crystalline and glassy phases. To reinforce this analogy we have investigated the behavior of a system initially prepared in an ordered configuration. Interestingly, we have found that in the region of low  $F$  and high  $\phi$ , where jamming was previously found, the ordered flow is not arrested and keeps going with a finite value of  $\eta$  (although the system might jam at times longer than those we can investigate). In the other regions of the flow diagram, on the contrary, the long time state of the system is that shown in Fig. 5c regardless of the initial conditions. This dependence on the initial conditions is analogous to that observed in thermal systems, where the crystalline phase is stable in the region where the glassy phase is found.

This work has been supported by EU Network MRTN-

CT-2003-504712.

- 
- \* Electronic address: denis.grebenkov@polytechnique.edu
- [1] J. B. Knight, C. G. Fandrich, C. N. Lau, H. M. Jaeger, and S. R. Nagel, Phys. Rev. E **51**, 3957 (1995).
  - [2] M. Nicodemi, A. Coniglio, H. J. Herrmann, Phys. Rev. E **55**, 3962 (1997).
  - [3] P. Richard, M. Nicodemi, R. Delannay, P. Ribière, and D. Bideau, Nature Materials **4**, 121 (2005).
  - [4] A. J. Liu, S. R. Nagel, Nature **396**, 21 (1998).
  - [5] A. Coniglio, A. Fierro, H. J. Herrmann, and M. Nicodemi (eds), Unifying Concepts in Granular Media and Glasses (Elsevier, Amsterdam, 2004).
  - [6] E. I. Corwin, H. M. Jaeger, and S. R. Nagel, Nature **435**, 1075 (2005).
  - [7] K. E. Daniels and R. P. Behringer, Phys. Rev. Lett. **94**, 168001 (2005).
  - [8] J.-C. Tsai, G. A. Voth, and J. P. Gollub, Phys. Rev. Lett. **91**, 064301 (2003).
  - [9] E. Bertrand, J. Bibette, and V. Schmitt, Phys. Rev. E **66**, 060401(R) (2002).
  - [10] D. J. Pine (talk, KITP Program on Granular Physics, 2005).
  - [11] L. E. Silbert, D. Ertas, G. S. Grest, T. C. Halsey, D. Levine, and S. J. Plimpton, Phys. Rev. E **64**, 051302 (2001).
  - [12] Distances, times, velocities, forces, elastic constants, and stresses are, respectively, measured in units of  $d$ ,  $t_0 = \sqrt{d/g}$ ,  $v_0 = \sqrt{gd}$ ,  $F_0 = mg$ ,  $k_n = mg/d$ , and  $\sigma_0 = mg/d^2$ , where  $g$  is gravity acceleration.
  - [13] P. G. Debenedetti and F. H. Stillinger, Nature **410**, 259 (2001).
  - [14] J.-C. Tsai and J. P. Gollub, Phys. Rev. E **70**, 031303 (2004). Phys. Rev. E **72**, 051304 (2005).
  - [15] R. L. Hoffman, J. Colloid Interface Sci. **46**, 491 (1974); J. J. Erpenbeck, Phys. Rev. Lett. **52**, 1333 (1984); R. L. Hoffman, J. Rheol. **42**, 111 (1998); B. J. Ackerson and P.N. Pusey, Phys. Rev. Lett. **61**, 1033 (1988); L. B. Chen *et al.*, Phys. Rev. Lett. **69**, 688 (1992).
  - [16] I. M. Krieger, Adv. Colloid Interface Sci. **3**, 111 (1972).
  - [17] M. E. Cates, J. P. Wittmer, J.-P. Bouchaud, and P. Claudin, Phys. Rev. Lett. **81**, 1841 (1998).
  - [18] R. S. Farr, J. R. Melrose, and R. C. Ball, Phys. Rev. E **55**, 7203 (1997).
  - [19] Due to the box rough boundaries (and finite size of the investigated system) the volume fraction definition has a degree of ambiguity. We use  $\phi = Nv_g/(l_x l_y l_z)$ , where  $v_g$  is the volume of a bead. Other definitions, as for instance  $\phi' = Nv_g/(l_x l_y l_z - V_b)$ , where  $V_b$  is the volume of the beads forming the rough boundaries, may differ up to 10%.